Paper published in:

A.W. Bruno, D. Gallipoli, C. Perlot, H. Kallel (2020).

Thermal performance of fired and unfired earth bricks walls.

Journal of Building Engineering, 28: 101017

https://doi.org/10.1016/j.jobe.2019.101017

THERMAL PERFORMANCE OF FIRED AND UNFIRED EARTH BRICKS WALLS

Agostino Walter Bruno[1], Domenico Gallipoli[2], Céline Perlot[2] and Hatem Kallel[2]

[1] School of Engineering, Geotechnics and Structures, Newcastle University, United Kingdom

[2] Université de Pau et des Pays de l'Adour/E2S UPPA, Laboratoire des Sciences de l'Ingénieur Appliquées à la Mécanique et au Génie Electrique- IPRA, EA4581, 64600, Anglet, France

DATE OF SUBMISSION: 17/09/2019

NUMBER OF WORDS: 5235

NUMBER OF TABLES: 3

NUMBER OF FIGURES: 13

CORRESPONDING AUTHOR: Agostino Walter BRUNO
Newcastle University
School of Engineering
Geotechnics and Structures
Devonshire Terrace
Drummond Building, Room 1.05
NE1 7RU, Newcastle upon Tyne
United Kingdom
e-mail: agostino.bruno@newcastle.ac.uk

ABSTRACT:

The paper presents the results from a series of thermal tests on five wall samples made of four types of unfired and one type of fired earth bricks. The unfired earth bricks were manufactured in the present work and consisted of Proctor compacted full bricks, hypercompacted full bricks, hypercompacted full bricks with hemp fibres and hypercompacted hollow bricks. Instead, the fired earth bricks were standard full bricks purchased from a provider of building materials. The walls were laid by using a fine earth mortar in the case of the unfired bricks and a standard cement mortar in the case of the fired bricks. The walls were tested inside a double-room climatic chamber where they were subjected to different temperatures on their two faces reproducing typical indoor and outdoor conditions. The thermal efficiency of the walls was assessed by quantifying the heat exchanged between the indoor and outdoor environments under both winter and summer testing conditions. The best thermal efficiency was observed for the unfired hypercompacted hollow brick wall while the worst efficiency was observed for the unfired hypercompacted and fired full bricks walls. An intermediate efficiency was recorded for the walls made of unfired full bricks either lightly compacted or hypercompacted with hemp fibres. The results from the present campaign provide an experimental database for the validation of heat transfer models at structural scale, thus contributing to the promotion of raw earth as a sustainable construction material.

KEYWORDS: Thermal performance; Energy consumption; Heat flux; Earth material; Masonry wall; Building envelope.

INTRODUCTION

According to the International Energy Agency (IEA, 2013), the building sector consumes about 32% of the global energy demand. About 37% of this energy consumption is spent to heat or cool indoor spaces (Fahmy et al., 2014; Fang et al., 2014; Stazi et al., 2014; Karimpour et al., 2015; Serrano et al., 2016) and strongly depends on the thermal efficiency of the building envelopes (Aste et al., 2009; Wang et al., 2009; Mirrahimi et al., 2016). A thermally insulating envelope can significantly reduce indoor heat losses during winter and indoor heat gains during summer (Soudani et al., 2016), thus reducing the energy spent for the air conditioning of dwellings.

Raw (unfired) earth constitutes a sustainable construction material that can help reducing the environmental impact of dwellings. Raw earth can be locally sourced and put in place with very little transformation, thus minimising embodied energy (Little and Morton, 2001; Morel et al., 2001). Raw earth can also be easily recycled or safely disposed into the environment at the end of service life, thus reducing the amount of hazardous demolition waste. On a negative note, dense earth exhibits a high thermal conductivity (Hall and Allinson, 2009; Cagnon et al., 2014; Maillard and Aubert, 2014; Indekeu et al., 2017; Dao et al., 2018) compared to other insulating materials (Papadopoulos, 2005). This unfavourable property is however partly compensated by a relatively large hygro-thermal inertia, which enables earth walls to act as moisture and heat buffers. Earth walls can therefore smooth out the indoor fluctuations of humidity and temperature, thus reducing heating and cooling needs (Houben and Guillaud, 1989; Allinson and Hall, 2010; Pacheco-Torgal and Jalali, 2012; McGregor et al., 2014; Soudani et al., 2016; Gallipoli et al., 2017; Soudani et al., 2017). The large hygro-thermal inertia of raw earth originates from its fine network of nanopores (i.e. pores with a diameter smaller than 10 nm) and from the high specific surface of the clay fraction (McGregor et al., 2016), which enhance the tendency of this material to adsorb and release vapour from humid and dry environments, respectively, while liberating and storing latent heat.

Many studies have measured the thermal properties of raw earth at the material scale (e.g. Hall and Allinson, 2009; Maillard and Aubert, 2014; Dao et al., 2018; Tinsley and Pavia, 2019) but only a handful of them have characterised the behaviour at the wall scale. Among these few studies, some have tested wall samples in the laboratory (e.g. Hall and Allison, 2010; Li et al., 2015; Medjelekh et al., 2016; Serrano et al., 2016) while others have monitored the behaviour of real walls in situ (e.g. El Fgaier et al., 2015; Soudani et al., 2017). To the best of the Authors' knowledge, a comparative assessment of the thermal performance of masonry walls made of different types of unfired or standard fired earth bricks has never been presented in literature.

To overcome this limitation, this paper presents a laboratory campaign of thermal tests on five wall samples made of four different types of unfired earth bricks and one type of fired earth brick. The four unfired earth brick types were manufactured in the present work and consisted of Proctor (i.e. lightly compacted) full bricks, hypercompacted full bricks, hypercompacted full bricks incorporating hemp fibres and hypercompacted hollow bricks. Standard fired full bricks were instead purchased from a provider of building materials and offered a reference for comparison with the unfired bricks. Two different types of mortars, namely a fine earth mortar and a standard cement mortar, were employed for manufacturing the unfired and fired bricks walls, respectively.

All walls were tested inside a double-room climatic chamber that allowed the application of different temperatures on the two wall faces to reproduce typical indoor and outdoor conditions. Two distinct sets of indoor and outdoor conditions were considered to replicate winter and summer climates. During the tests, the thermal efficiency of the walls was assessed by measuring the amount of heat exchanged between the indoor and outdoor environments. Results show that the unfired hypercompacted hollow brick wall enables the lowest heat flux between indoor and outdoor environments while the walls made of either unfired hypercompacted or standard fired full bricks allow the highest heat flux. The inclusion of hemp fibres and the application of a lighter compaction effort markedly improve the behaviour of the unfired full bricks resulting in an intermediate level of

thermal efficiency. Interestingly, the outcomes of this study are relevant to practitioners and stakeholders working on the energy efficiency of buildings with a focus in façades and envelope engineering.

MATERIALS AND METHODS

Four types of unfired earth bricks were manufactured in the present work from an illitic soil containing 0.4% gravel, 40.4% sand, 42.9% silt and 16.3% clay as determined by wet sieving and sedimentation tests in compliance with the norms XP P94-041 (AFNOR, 1995) and NF P94-057 (AFNOR, 1992). Plasticity tests were also performed on the soil fraction smaller than 400 μm, in compliance with the norm NF P94-051 (AFNOR, 1993), showing a liquid limit of 33.0%, a plastic limit of 20.1% and, hence, a plasticity index of 12.9%. Finally, the soil grains have a specific gravity of 2.66, which has been determined as the average of three pycnometer tests conducted according to the norm NF P 94-054 (AFNOR, 1991).

The unfired earth bricks were compacted along their shortest dimension inside a stiff mould (Bruno et al., 2017a) with a size of 200 x 100 x 50 mm^3. The fired earth bricks were instead purchased from a commercial provider of building materials and had a slightly larger size of 220 x 110 x 50 mm^3. A brief description of the manufacturing process for all five brick types is given below.

- *Unfired lightly compacted full bricks (hereafter named "Proctor bricks")*

  Dry earth was first mixed at a water content of 13.5%, which is the optimum water content of standard Proctor compacted earth as determined by the norm NF P 94-093 (AFNOR, 1999). The moist earth was subsequently stored inside two plastic bags for at least 24 hours to ensure the equalisation of pore water pressures. The equalised earth was then one-dimensionally compacted inside the brick mould by a piston with a displacement rate of 0.1 mm/s until the desired height of 50 mm was attained. The amount of earth placed inside the mould was calculated to attain a final dry density of 1860 kg/m^3, which corresponds to the optimum dry density of standard Proctor compacted earth.

- *Unfired hypercompacted full bricks (hereafter named "hypercompacted bricks")*

  "Hypercompaction" is the method of manufacturing unfired earth bricks described in Bruno et al. (2017a) and Bruno (2016). The method consists in the one-dimensional compaction of the earth to an ultimate pressure of 100 MPa with a loading rate of 0.17 MPa/s. The earth is "double compacted" by two pistons acting at the top and bottom of a "floating" mould supported by internal friction against the brick surface. Double compaction is preferable to single compaction because it reduces the effect of friction on the brick surface and therefore increases the uniformity of stress and porosity inside the material. Note that double compaction can only be employed for hypercompacted bricks because, for Proctor bricks, the applied pressure is too low to generate enough lateral friction to support the weight of the mould. The bricks were hypercompacted at a water content of 5.2%, which is the optimum water content of the hypercompacted earth as determined by Bruno et al. (2017a). Prior to hypercompaction, the earth was mixed with the required amount of water and stored inside two plastic bags for at least 24 hours to achieve equalisation of pore water pressures. This manufacturing process generated a closely packed material with a relatively high dry density of 2320 kg/m^3 and, hence, a low porosity of only 0.129.

- *Unfired hypercompacted full bricks including hemp fibers (hereafter named "hemp bricks")*

  The dry earth was mixed, together with 1.5% of hemp fibres mass, at a water content of 5.4%, which is the optimum water content of the hypercompacted earth incorporating hemp fibres. A relatively small amount of only 1.5% of fibres was chosen to facilitate mixing and hypercompaction of the material.

  The optimum water content was determined by hypercompacting earth-hemp samples at different water contents and is slightly higher than the optimum water content of the hypercompacted earth without hemp because of moisture absorption by the fibres. Table 1 lists the main properties of the hemp fibres as stated by the company "Technichanvre", which is the seller of these fibres.

Table 1. Main properties of hemp fibres

Fibre length	1-5 mm
Dry density	130 – 140 kg/m^3
Thermal conductivity (dry condition)	0.048 W/mK
Water retention capacity	370 ml/l

The moist earth-hemp mix was stored inside two plastic bags for at least 24 hours to attain equalisation before being hypercompacted to 100 MPa resulting in a dry density of 2244 kg/m^3 and a porosity of 0.150. Note that these values of density and porosity have been calculated by using the weighted average of the specific gravities of the soil and hemp fibres. In particular, the specific gravity of the hemp fibres has been taken equal to 1.39 according to the experimental work of Rohen et al. (2017).

Hemp bricks are therefore only slightly less dense than hypercompacted bricks because of the very small amount of added fibres. The similarity of the dry densities of these two bricks allows isolating the effect of the fibres from that of the porosity.

- *Unfired hypercompacted hollow bricks (hereafter named "hollow bricks")*

  Dry earth was mixed at the optimum water content of 5.2% and then stored inside plastic bags for 24 hours to attain equalisation of pore water pressures before being hypercompacted to 100 MPa. The bricks were double compacted by using a set of specifically designed pistons to create two 55 mm diameter cylindrical holes perpendicular to the largest brick face. The presence of these two holes resulted in an apparent dry density (defined as the ratio between the dry mass and the overall brick volume including the two holes) of about 1770 kg/m^3. Note that the actual dry density of the earth is identical to that of hypercompacted bricks as both these bricks are made of the same material.

- *Fired extruded full bricks (hereafter named "fired bricks")*

  Fired earth bricks were purchased from a commercial provider (Castorama – product code 8715098067447), which unfortunately did not share the details of the manufacturing process. In general terms, the manufacture of the fired bricks involved first grinding the

earth to a uniform size. The ground earth was subsequently mixed with a high water amount to produce a paste that was extruded through a rectangular ejector with a size of 110 x 50 mm^2. The extruded strip was then cut into individual bricks, each having a length of 220 mm. The freshly cut bricks were dried and subsequently fired to a temperature of about 1100 ˚C for a time between 10 and 40 hours. More information about the standard procedures for the manufacture of fired earth bricks can be found in the technical notes published by the Brick Industry Association (2006).

Figure 1 shows the five brick types tested in the present work together with their dimensions in millimetres.

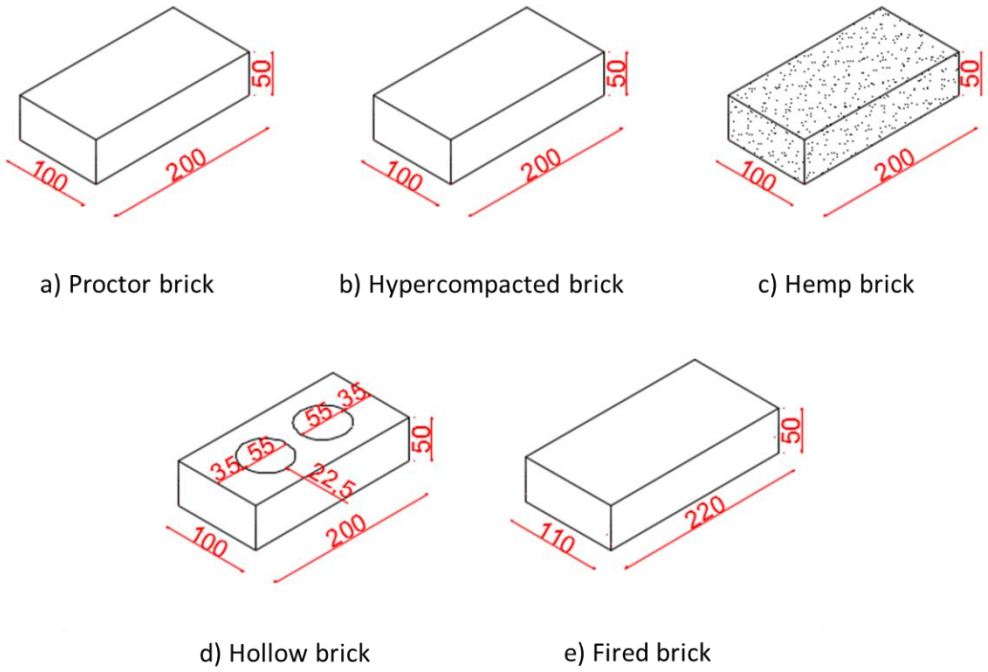

Figure 1. Representation of the five brick types tested in the present work: a) unfired lightly compacted full brick (Proctor brick), b) unfired hypercompacted full brick (hypercompacted brick), c) unfired hypercompacted full brick including hemp fibers (hemp brick), d) unfired hypercompacted hollow bricks (hollow brick) and e) fired extruded full brick (fired brick)

Prior to testing, all bricks were equalised to the laboratory atmosphere corresponding to a temperature of about 25 °C and a relative humidity of about 40% for a minimum of two weeks and, in any case, until a constant mass was attained. After equalisation, the water content of all types of brick was measured according to the norm NF P 94-050 (AFNOR, 1995). All four unfired bricks attained similar water contents, just above 3%, while the water content of the fired brick remained close to zero, which reflects the greater hygroscopicity of the unfired earth compared to the fired earth.

Table 2 summarises the main physical properties of the five bricks after equalisation. Recall that the densities and porosity of the hollow bricks indicated in Table 2 are the apparent ones, i.e. they have been calculated by considering the two holes in the same way as material pores. The actual earth densities and porosity of the hollow bricks are instead identical to those of the hypercompacted bricks as these two bricks are made of the same material

Table 2. Bulk density, dry density, porosity and water content of the five bricks after equalisation

	Bulk density (kg/m^3)	Dry density (kg/m^3)	Porosity (-)	Water content (%)
Proctor	1927	1863	0.300	3.41
Hypercompacted	2397	2320	0.129	3.34
Hemp	2316	2244	0.150	3.22
Hollow[1]	1828	1770	0.336	3.29
Fired	2026	2025	0.240	0.06

[1]For hollow bricks, the indicated densities and porosity are the apparent ones, i.e. they have been calculated considering the two holes in the same way as material pores. The actual earth densities and porosity are instead identical to those of the hypercompacted bricks.

Inspection of Table 2 indicates that the tested bricks cover a large range of dry densities (from 1770 to 2320 kg/m^3) and porosities (from 0.129 to 0.336). These values are comparable to those of most construction materials including, for example, lightweight to dense aggregate concrete blocks (The Concrete Block Association, 2017).

Prior to manufacturing the wall samples, the thermal conductivities of the different brick materials were measured under different humidity conditions. In particular, the bricks were equalised at three different levels of relative humidity, i.e. 25%, 62% and 95%, under a constant temperature of 23 ˚C before measuring the thermal conductivity by means of a hot disk apparatus. Three different measurements were taken at each level of relative humidity on a single sample of every brick type to evaluate the repeatability of results. Figure 2 shows the average values of thermal conductivity from the three test repeats together with the corresponding standard deviations. The standard deviation bars are barely visible in Figure 2 due to the high repeatability of the obtained results. The same thermal conductivity is shown for both hypercompacted and hollow bricks because these two bricks are made of the same material.

Inspection of Figure 2 indicates that the material of the hypercompacted and hollow bricks exhibits the largest thermal conductivity due to its very low porosity. A lower conductivity is instead displayed by the material of the unfired hemp bricks thanks to the presence of insulating fibres, despite an ostensibly similar porosity. An even lower conductivity is exhibited by the material of the unfired Proctor bricks due to insulating effect of the larger porosity. Interestingly, the fired bricks exhibit the lowest thermal conductivity of all bricks, even lower than that of the Proctor bricks, which have however a higher porosity than the fired bricks. This could be the consequence of the particular pore size distribution of the fired earth or a significantly lower conductivity of the solid phase following mineralogical changes during firing. Inspection of Figure 2 also indicates that, among all unfired materials, the material of the Proctor bricks exhibits the highest sensitivity to variations of relative humidity. This is because of the large porosity of this material, which implies a relatively high capacity to store or release moisture during changes of ambient humidity. The thermal conductivity of the fired bricks is instead virtually unaffected by the variations of ambient humidity due to the limited capacity of this material to store or release moisture (Rode et al., 2005; Bruno et al., 2019). This is consistent with the data shown in Table 2, which indicate that the fired bricks only store negligible amounts of water upon equalisation to the laboratory atmosphere.

Overall, the values of thermal conductivity measured on hypercompacted and Proctor bricks are consistent with results from past studies on unfired earth bricks compacted at different levels of dry density (e.g. Cagnon et al., 2014; Soudani et al., 2017). The thermal conductivity measured on hemp bricks is instead higher than that usually found in literature on similar materials (e.g. Laborel-Préneron et al., 2018; Mazhoud et al., 2018) and this is due to the high density of hemp bricks in the present study. Finally, the thermal conductivity of standard fired bricks well matches existing values in literature (e.g. Dondi et al., 2004)

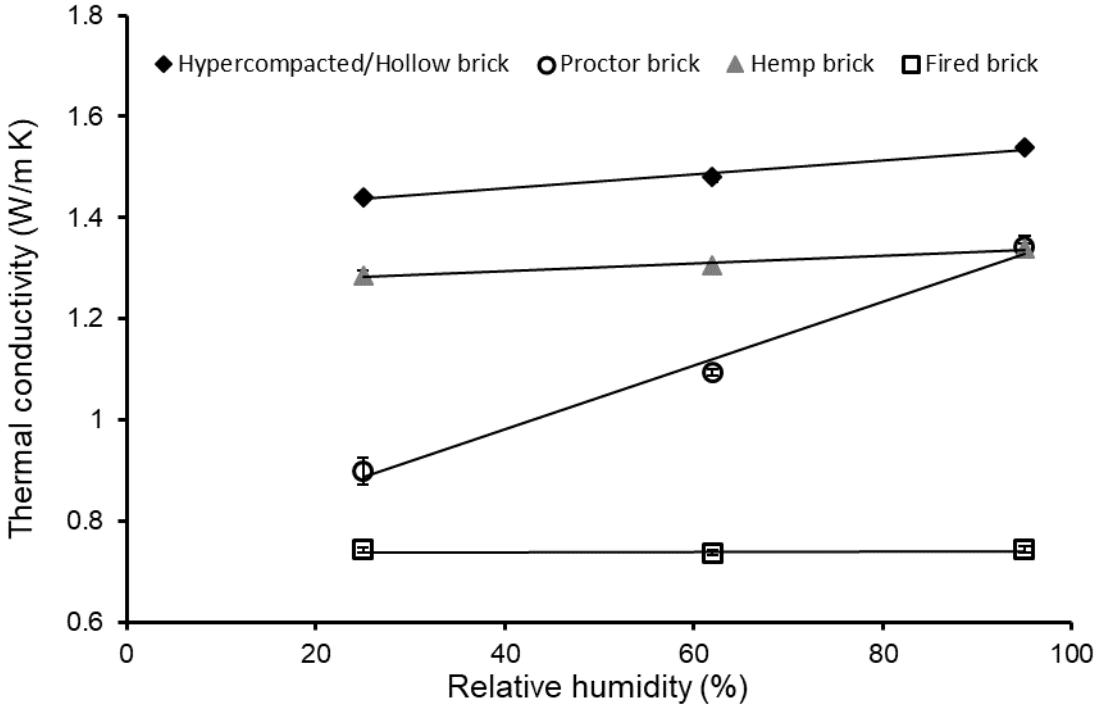

Figure 2. Variation of thermal conductivity with ambient relative humidity for the different materials of hypercompacted, hollow, Proctor, hemp and fired bricks

Next, the thermal performance of the five wall samples was tested by using a double-room climatic chamber. Four unfired bricks walls (i.e. walls made of Proctor, hypercompacted, hemp and hollow bricks) were laid by using a fine earth mortar while one fired brick wall was laid by using a conventional cement mortar. The fine earth mortar was produced from the finest earth fraction, i.e. the fraction passing through the 400 µm sieve, which was first oven dried to 105 °C for at least 24 hours and then mixed with a water content of 26.6%. This water content, which corresponds to the

average of the liquid and plastic limits, was chosen to ensure a good workability of the mortar during fabrication of the wall. The cement mortar consisted instead of a standard mix of cement, sand and water in the proportions of 1:3:0.5 by weight (Li et al., 2004; AFNOR, 2006) as commonly used for the construction of masonry walls.

The same laying method was adopted to build all wall samples regardless of the brick and mortar types. The brick surfaces were first slightly wetted with a moist cloth and then joined together with a 10 mm thick mortar layer. Each wall was made of ten brick layers with each layer composed of two entire bricks plus a dry-sawn brick portion positioned alternatively at opposite sides to avoid continuous vertical mortar joints. This laying method produced wall samples with a vertical surface of about 520 x 590 mm^2 and a thickness of 100 mm, except for the wall made of fired bricks, which had a slightly larger thickness of 110 mm. Note that measurements of heat flux across the fired brick wall were scaled up by a factor of 1.1 to account for the larger thickness of this particular wall and therefore to enable comparison with the other four unfired earth walls. Figure 3 shows a schematic representation of the five walls tested in the present work together with the corresponding dimensions in millimetres.

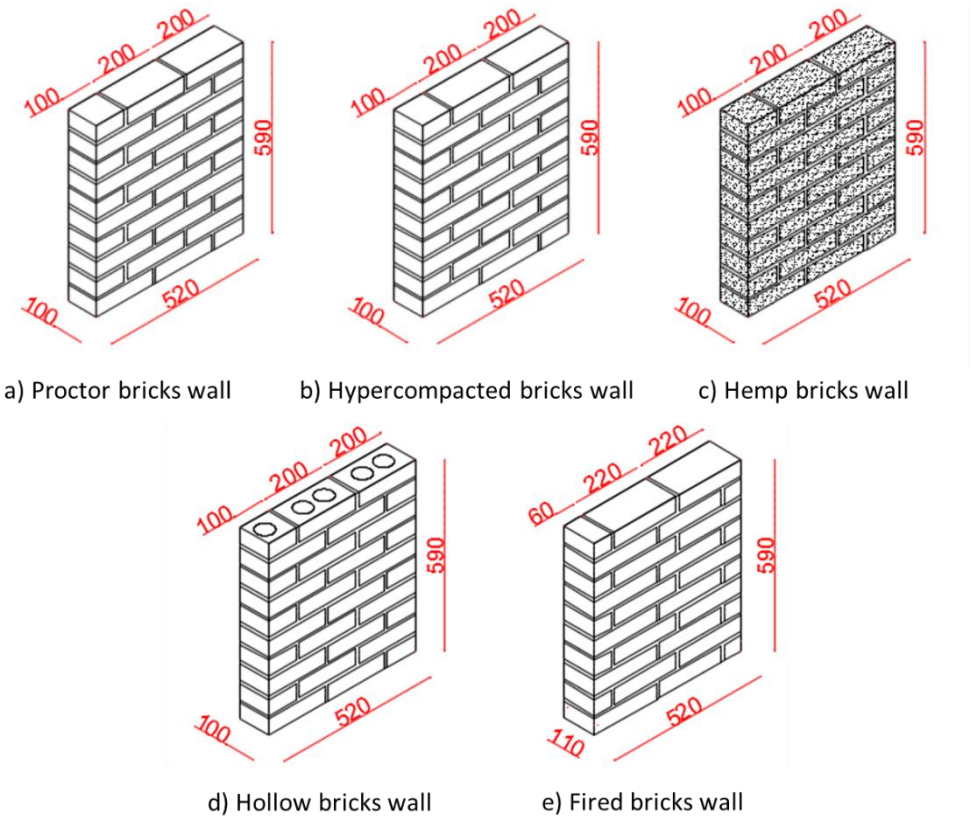

Figure 3. Representation of the five walls tested in the present work: a) Proctor brick wall, b) hypercompacted brick wall, c) hemp brick wall, d) hollow brick wall and e) fired brick wall.

Prior to thermal testing, all walls were equalised to the laboratory atmosphere, corresponding to a temperature of about 25 °C and a relative humidity of about 40%, for a minimum time of two weeks. After equalisation, the wall samples were placed inside the testing frame of the climatic chamber and the small gap between the perimeter of the wall and the inner edge of the frame was filled with insulating glass wool before being covered by aluminium tape (Figure 4). This ensured that thermal exchanges could only take place through the exposed wall surface. The testing frame was then sandwiched between the hot and cold rooms of the climatic chamber and thermally sealed from the laboratory environment by means of a clamping mechanism (Figure 5).

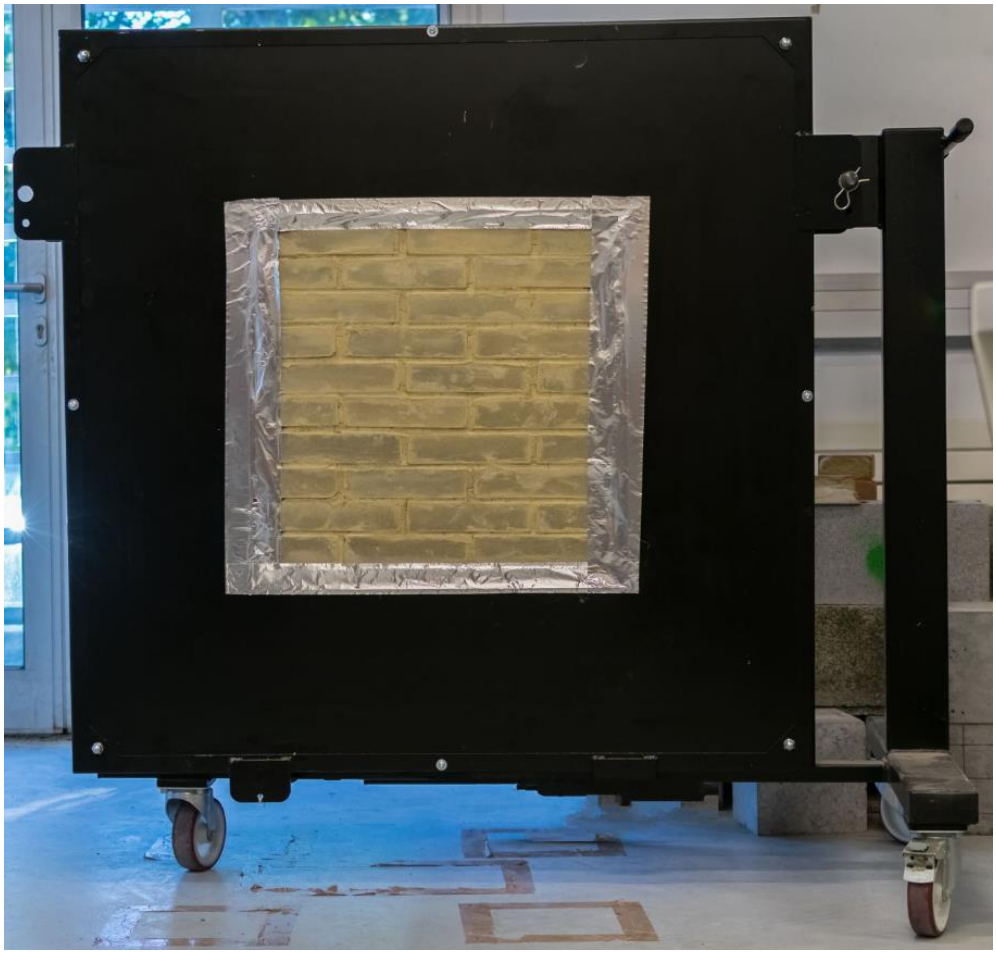

Figure 4. Hypercompacted brick wall inside the testing frame.

Figure 5. Testing frame containing the wall sample sealed between the hot and cold rooms of the climatic chamber.

PROCEDURE OF THERMAL TESTS ON WALL SAMPLES

The thermal tests on the wall samples were performed by using the "Thermo^{3}" double-room climatic chamber manufactured by the company "Recherches & Realisation Remy 3R". This climatic chamber is composed of two separate units, i.e. a hot and a cold room, which are thermally insulated from the external environment. During any given test, the temperature of the hot room is always higher than the temperature of the cold room, which generates a unidirectional flux of heat across the interposed wall. The climatic chamber is equipped with twenty sensors to measure the temperature of both the hot and cold rooms as well as the temperature of the two wall faces. Figure 6 shows a

horizontal cross-section of the climatic chamber, which also indicates the position of all temperature sensors.

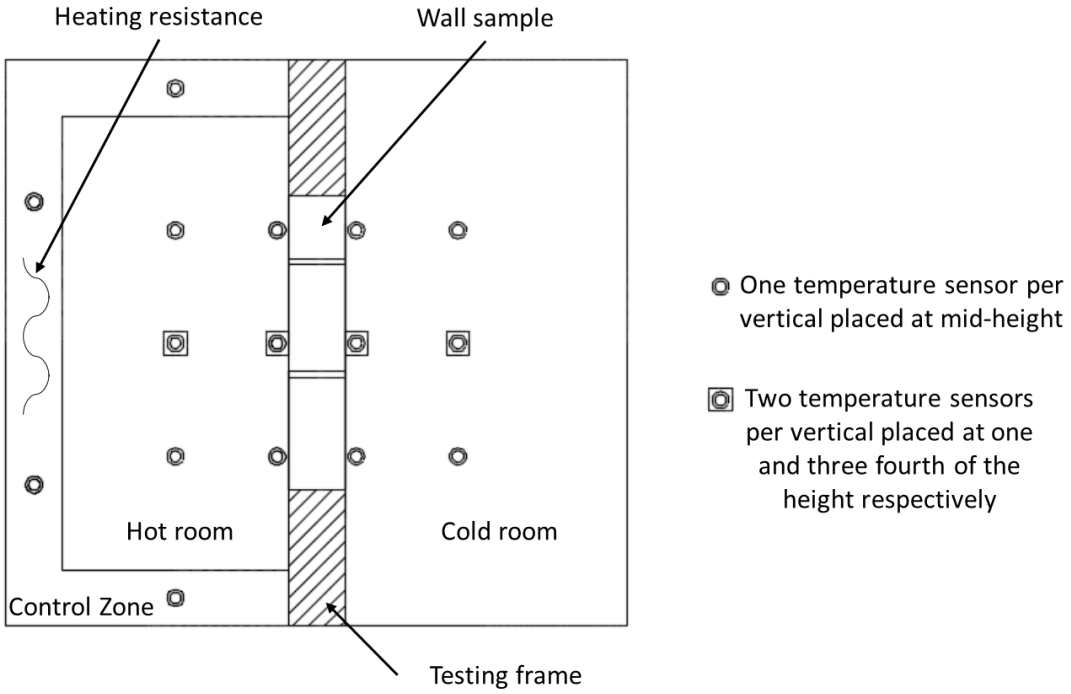

Figure 6. Schematic horizontal cross-section of the climatic chamber with indication of the temperature sensors.

The temperature of the hot room is regulated by a heating resistance located in the outer control zone (Figure 6). This resistance releases a known amount of energy whenever heat is lost through the wall from the hot room towards the cold room. The resistance is automatically activated when the temperature of the hot room drops more than 0.3 ˚C below the target and is stopped when this temperature exceeds the target by more than 0.3 ˚C. The equipment records this intermittent release of energy, which is then averaged to estimate the continuous heat flux through the wall. Unfortunately, the hot room is not equipped with a refrigerator system, which implies that the temperature can only be increased or kept constant but never decreased. Conversely, the cold room

is equipped with a reversible system comprising both a heating resistance and a refrigerator, which allows the imposition of temperature cycles.

Each wall sample was subjected to two distinct tests with the aim of simulating typical conditions during both winter and summer seasons. A brief description of these two testing conditions is provided in the following.

- *Simulation of winter condition*

  The wall samples were exposed to a constant hot room temperature of 23 ˚C, which reproduced indoor comfort conditions, and to a cold room temperature varying between 5 ˚C and 15 ˚C with a 24-hours sinusoidal cycle, which reproduced the daily fluctuation of outdoor climate. This testing condition, which is graphically represented in Figure 7, was maintained for one week while the energy released by the resistance was measured to infer heat losses through the wall.

- *Simulation of summer condition*

  A constant cold room temperature of 23 ˚C was maintained to reproduce the same indoor comfort conditions as during winter, while the hot room temperature was increased in six stages to 25, 28, 31, 34, 37 and 40 ˚C to reproduce increasingly warmer outdoor climates. Each temperature stage was maintained during 48 hours, which allowed the achievement of a steady state regime corresponding to the measurement of a constant heat flux through the wall over a period of at least 24 hours. Note that a sinusoidal variation of temperature could not be applied under summer conditions as the hot room of the climatic chamber is only equipped with a heating resistance without any refrigerator. Hence, the temperature inside the hot room can either be increased or maintained constant but never decreased. Figure 8 provides a graphical representation of the imposed temperatures in both the hot and cold rooms.

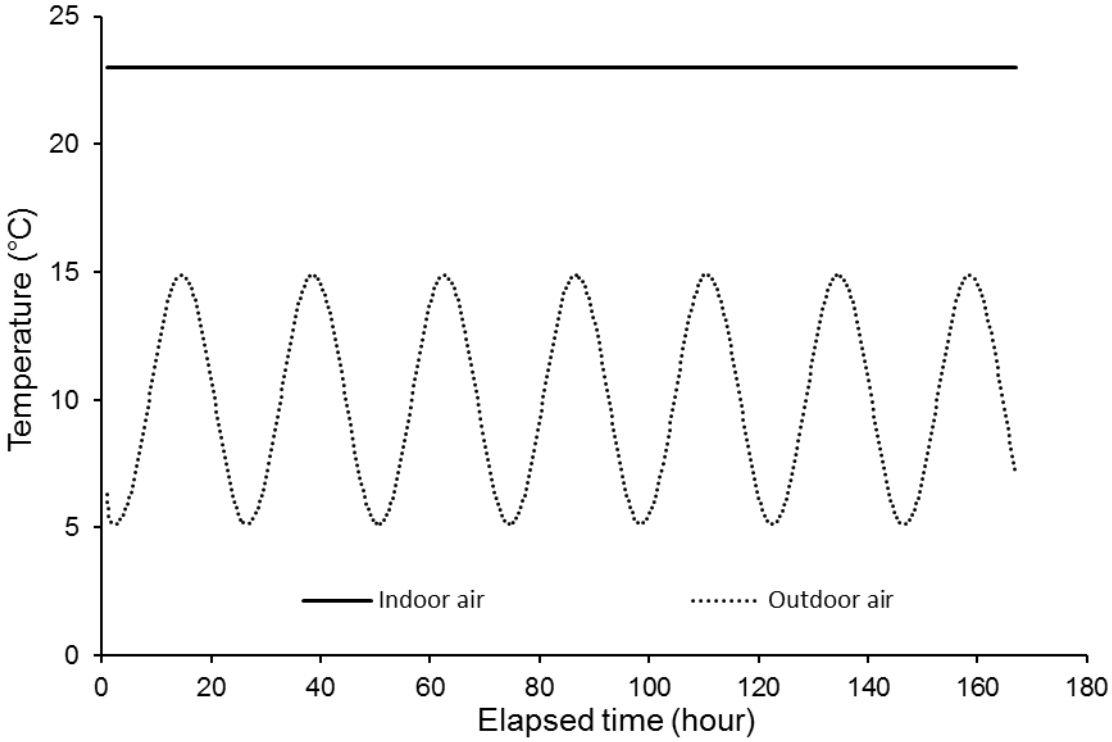

Figure 7. Winter testing conditions.

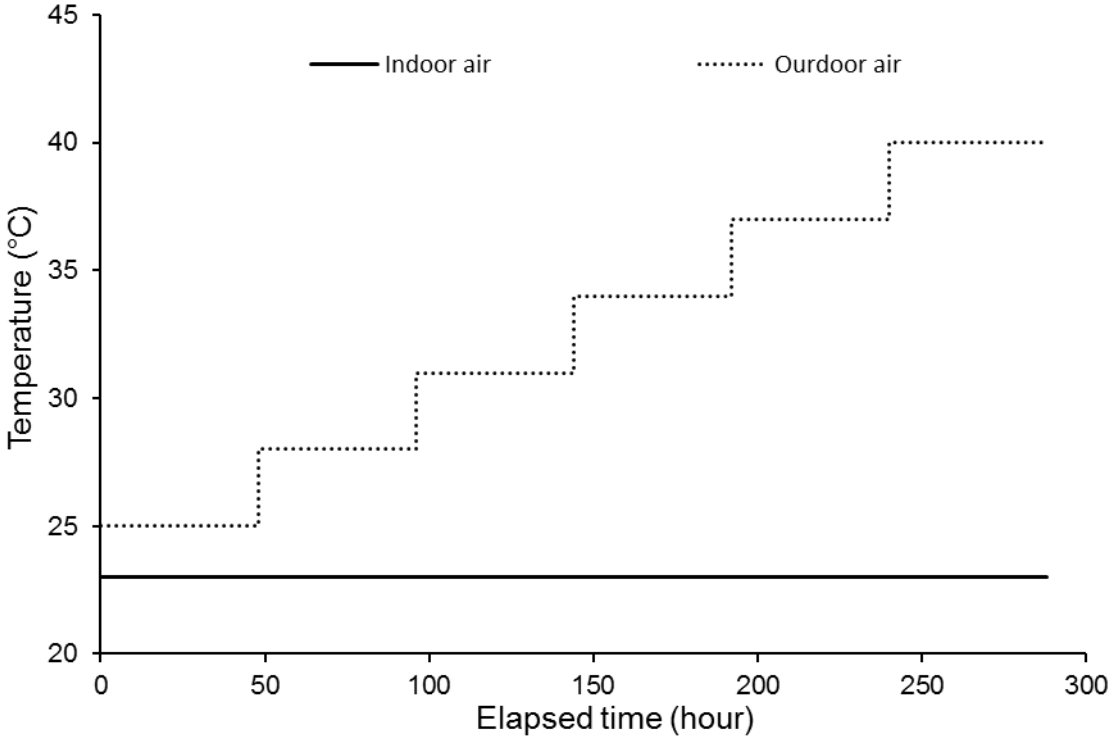

Figure 8. Summer testing conditions.

RESULTS OF THERMAL TESTS ON WALL SAMPLES

During the tests on the wall samples, a data logger continuously recorded: a) the energy released by the resistance to compensate the heat flux through the wall and b) the temperature of the two wall faces.

Winter testing conditions

Under winter testing conditions, the indoor heat losses were measured from the energy released by the heating resistance to maintain an indoor temperature of 23 ˚C while the outdoor temperature varied cyclically between 5 and 15 ˚C. Figure 9 shows that the heat flux across the wall is not constant but fluctuates like the outdoor temperature over a 24-hour period and it attains a peak when the thermal gradient across the wall is largest. Interestingly, the phase of the heat flux cycles is identical for all tested walls and matches well the phase of the outdoor temperature cycles.

Inspection of Figure 9 also indicates that the heat flux across the five wall samples is similar when the temperature difference between the two rooms is smallest and equal to 8 ˚C (corresponding to an indoor temperature of 23 ˚C and an outdoor temperature of 15 ˚C). The only exception to this behaviour is given by the hollow brick wall that shows a consistently lower heat flux throughout the entire test. The dissimilarities between wall samples become however more evident as the thermal gradient across the wall increases and they are clearest when the temperature difference attains the maximum value of 18 ˚C (corresponding to an indoor temperature of 23 ˚C and an outdoor temperature of 5 ˚C). In this case, both the hypercompacted and fired bricks walls exhibit the largest heat flux, and hence the worst thermal efficiency. At the other end of the spectrum, the hollow brick wall exhibits the lowest heat flux and hence the best thermal efficiency. Given that hollow and hypercompacted bricks are made of the same material, the higher thermal efficiency of the hollow brick wall is entirely ascribed to the insulation provided by the air pockets inside the cylindrical holes. Note that, for the hollow brick wall, heat is also transferred by air convection occurring inside

the cylindrical holes, but this mechanism of heat transfer is rather weak compared with the high thermal resistance of the air pockets respect to the mechanism of heat conduction.

Similar to the conductivity measurements at material scale, the hemp and Proctor bricks walls exhibit an intermediate level of efficiency. Both these walls are also made of full bricks, which however incorporate either insulating fibres or larger porosity, with a consequent reduction of thermal conductivity compared to the hypercompacted bricks.

A special comment deserves the similar behaviour of the hypercompacted and fired bricks walls. This similarity may surprise as it contradicts previous measurements of thermal conductivity at material scale, which indicate a very different behaviour for the fired and hypercompacted bricks. In particular, the materials of the fired and hypercompacted bricks exhibit the lowest and highest values of thermal conductivity, respectively (Figure 2). This similar behaviour at the wall scale can however be explained by the occurrence of water condensation in the pores of the unfired earth but not in the pores of the fired earth (Bruno et al., 2017b; Bruno et al, 2018; Rode et al., 2005; Bruno et al., 2019). Water condensation is an exothermic process that releases latent heat as temperature reduces while water evaporation is an endothermic process that stores latent heat as temperature increases. With reference to the present tests, the condensation of pore water at low temperatures results in the release of a significant amount of latent heat. This partly compensates the higher thermal conductivity of the unfired earth, thus resulting in a similar heat flux across both the hypercompacted and fired bricks walls.

Figure 10 shows the temperature measured on the wall faces exposed to the indoor (solid lines) and outdoor (dotted lines) environments, respectively. Inspection of Figure 10 indicates a similar cyclic variation of the surface temperature for all wall samples, which is also in phase with the outdoor temperature cycles. This result suggests that the wall temperature mainly depends on the imposed environmental conditions rather than on the properties of the tested walls.

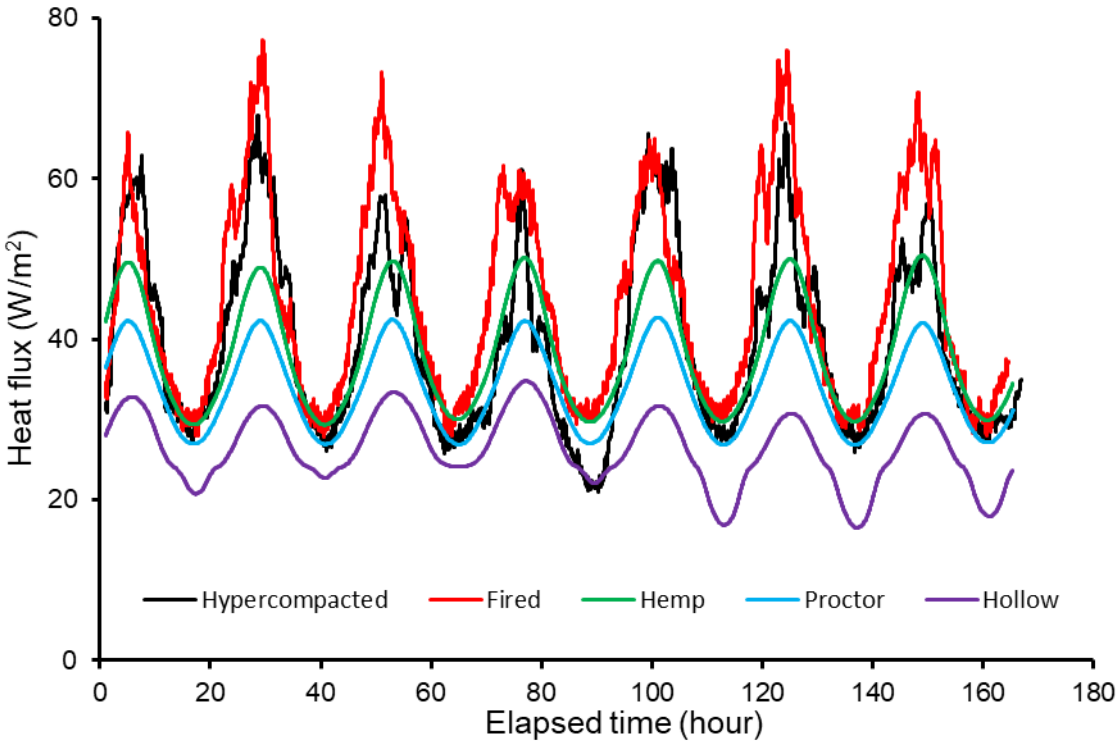

Figure 9. Heat fluxes across the tested walls under winter testing conditions.

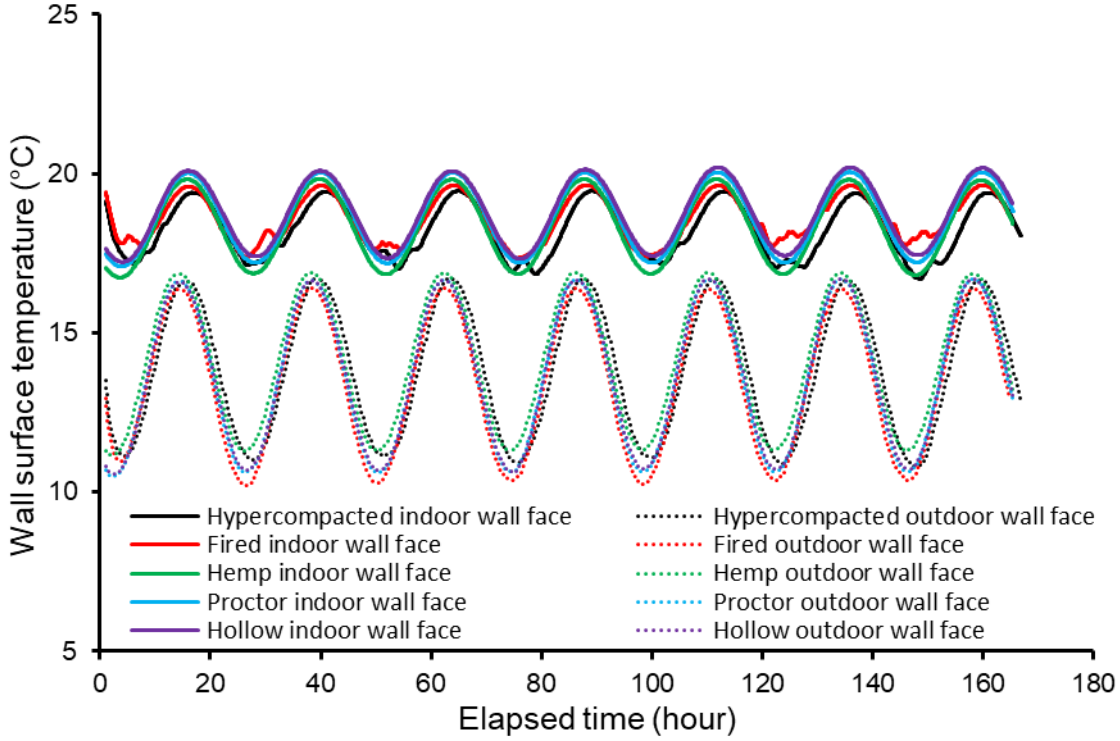

Figure 10. Wall surfaces temperatures under winter testing conditions.

Summer testing conditions

Under summer testing conditions, the indoor temperature was fixed at 23 ˚C while the outdoor temperature was increased in six different stages to 25, 28, 31, 34, 37 and 40 ˚C with each stage maintained for 48 hours. A time of 48 hours was enough to achieve steady state conditions corresponding to the measurement of a constant heat flux across the wall during at least 24 hours. The indoor heat gains were measured from the energy released by the resistance to control the outdoor temperature at the required level.

Figure 11 shows the steady state heat fluxes measured across all wall samples during the last 24 hours of each temperature stage. Similar to winter testing, the fluxes across the five walls are similar when the difference between indoor and outdoor temperatures is low but they start to diverge as the outdoor temperature becomes progressively higher and surpasses the indoor temperature by more than 8 ˚C.

Similar to winter testing, the hollow brick wall exhibits the lowest heat flux and therefore the best thermal efficiency due to the presence of insulating air pockets inside the brick holes. As for the full bricks walls, the results highlight once again the beneficial effect of water phase changes occurring in the unfired earth pores, but not in the fired earth pores, which may override the unfavourable influence of thermal conductivity. This is shown in Figure 11 where the fired brick wall exhibits one of the poorest thermal efficiencies despite displaying the lowest thermal conductivity according to Figure 2. This is due to the thermal inertia introduced by the evaporation of water stored in the unfired earth pores, which subtracts latent heat from the surrounding environment and therefore increases thermal efficiency in warmer climates.

However, when the outdoor temperature increases above 31 ˚C, the unfired earth becomes progressively drier and the beneficial effect of pore water evaporation tends to reduce. Thermal conductivity then regains prominence and the efficiency of the unfired earth walls starts to deteriorate in comparison to the fired earth wall.

Figure 12 shows the temperatures measured on the two wall faces exposed to the indoor (black markers) and outdoor (red markers) environments, respectively, after achieving steady state. Similar to winter testing, all walls display very similar temperatures on both faces, thus confirming that wall temperatures are mostly controlled by the imposed environmental conditions rather than by material properties.

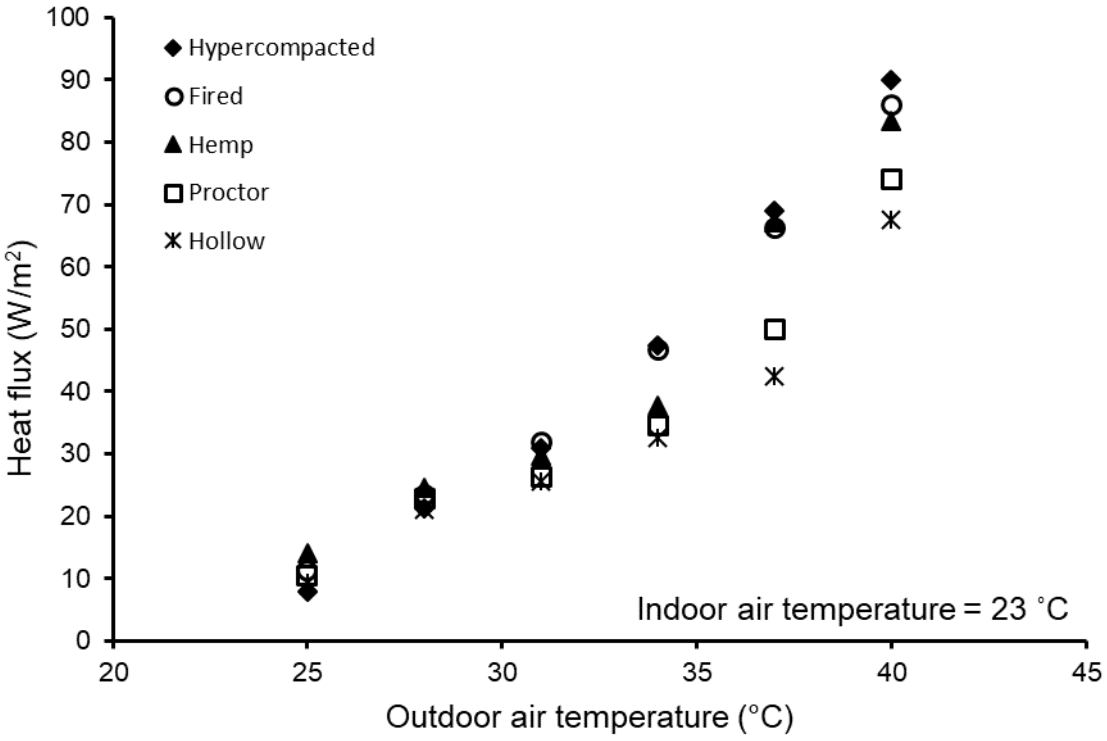

Figure 11. Heat fluxes across the tested walls under summer testing conditions.

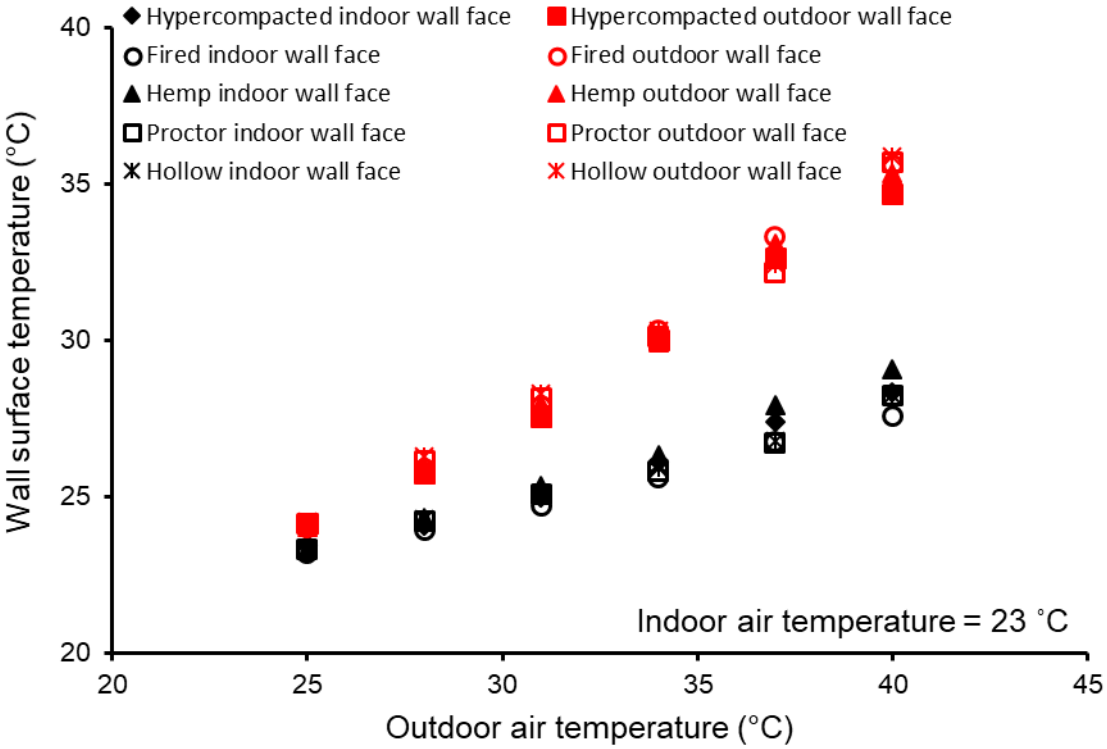

Figure 12. Wall surfaces temperatures under summer testing conditions.

Based on the experimental results shown in Figures 11 and 12, the values of heat flux are now plotted in Figure 13 against the gradient of temperature, which is the difference of temperature between the outdoor and indoor wall faces divided by the thickness of the wall. Note that, in Figure 13, the values of heat flux for the fired brick wall are those measured during testing without applying the scaling factor of 1.1. Interestingly, in Figure 13, the data for each tested wall are interpolated by a straight line that passes through the origin and with a slope equal to the thermal conductivity k of the wall according to the general equation of heat conduction:

$$q = -k\nabla T \tag{1}$$

Where q is the heat flux in $\frac{W}{m^2}$ and ∇T is the temperature gradient in $\frac{K}{m}$. Note that Equation (1) is valid under stationary conditions and hence the thermal conductivity of the tested walls cannot be determined under the transient testing conditions adopted to simulate a winter climate.

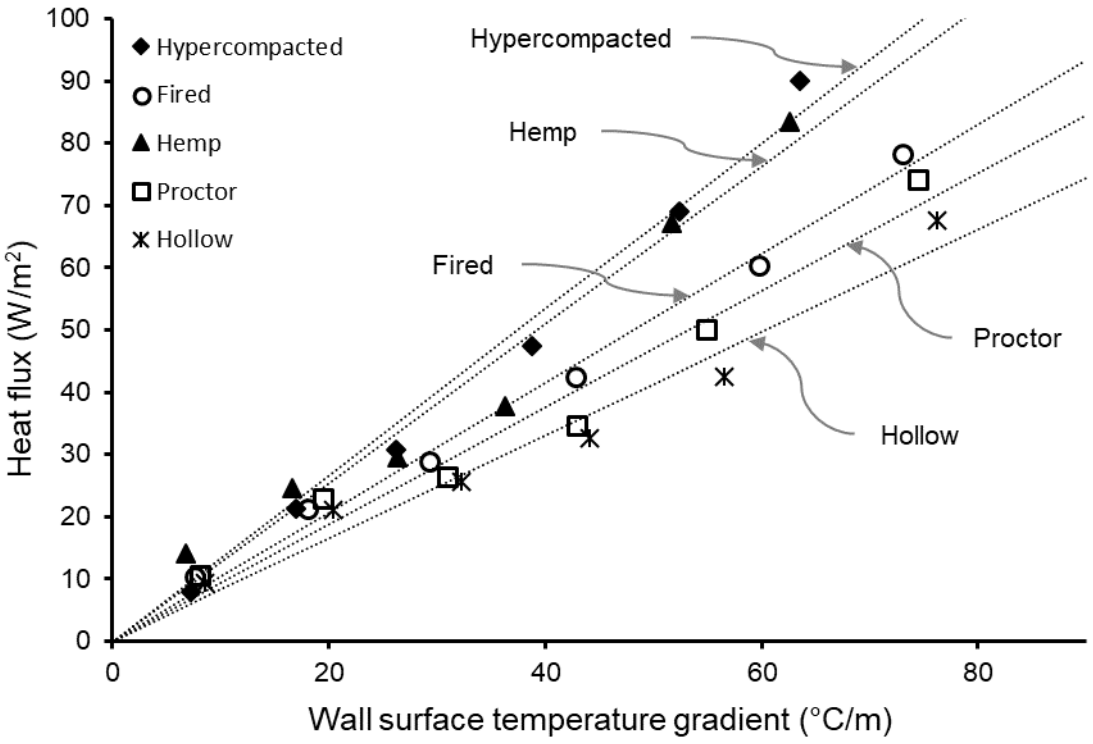

Figure 13. Heat flux across the tested walls against the gradient of temperature between indoor and outdoor wall faces.

The values of thermal conductivity of the tested walls, determined as the slope of the straight lines represented in Figure 13, are reported in Table 3 together with values of R^2 to indicate the excellent fit of the linear regressions. Inspection of Table 3 indicates that all tested walls exhibited a relatively small variation of thermal conductivity, which ranges from 0.83 to 1.33 $\frac{W}{m\,K}$. This implies that all tested walls exhibited a thermal performance which is rather similar at low temperature gradients and that tends to diverge as the temperature gradient grows, as represented by the diversion of the fitting straight lines in Figure 13.

Inspection of Table 3 finally indicates that the thermal conductivity of the hypercompacted brick wall is slightly lower than the one measured on the individual brick (Figure 2) and this is due to the presence of less compacted mortar joints with lower thermal conductivity. Hemp and Proctor brick walls exhibited instead a similar thermal conductivity to that of the corresponding individual bricks at low levels of relative humidity (Figure 2). This higher similarity can be associated to a more

homogenous thermal behaviour of individual bricks and mortar joints compared to the case of the hypercompacted brick wall. The hollow brick wall exhibited the lowest thermal conductivity and this is again related to the presence of low-conductive air pockets in the wall volume. Finally, the thermal conductivity of the fired brick wall is slightly higher than the one measured at the scale of the individual brick (Figure 2). This discrepancy can be related to the higher thermal conductivity of the cement mortar, which can reach values between 1.1 and 1.2 $\frac{W}{m\,K}$, as measured by Demirboğa (2003).

Table 3. Thermal conductivity of tested walls

	Thermal conductivity (W/m K)	R^2 (-)
Hypercompacted	1.33	0.986
Fired	1.04	0.992
Hemp	1.27	0.961
Proctor	0.94	0.965
Hollow	0.83	0.962

CONCLUSIONS

This paper has presented the results from a series of thermal tests on five different wall samples made of four types of unfired and one type of fired earth bricks. The tests have aimed to quantify the efficiency of the walls in minimizing indoor heat losses during winter and indoor heat gains during summer. The two wall faces were exposed to different ambient temperatures simulating typical indoor and outdoor conditions, respectively, while the heat flux across the wall was simultaneously measured. The main findings of the work can be summarised as follows:

- ***Effect of firing.*** The fired bricks exhibit lower thermal conductivity than all unfired earth bricks but their thermal efficiency at the wall scale is poorer than that of three out of four unfired earth bricks. This apparent contradiction is explained by the incapacity of fired earth, unlike unfired earth, to exchange pore water with the surrounding environment. Pore water exchanges correspond to the storage or release of latent heat depending on whether evaporation occurs in cold climates or condensation occurs in warm climates. Pore water

exchanges can therefore contribute to an increase of thermal inertia and hence result in a gain of thermal efficiency at the wall scale.

- ***Effect of dry density.*** The hypercompacted unfired full bricks exhibit, together with the fired full bricks, the poorest thermal performance at the wall scale. This is because the hypercompaction of the earth produces an extremely dense material with a very high thermal conductivity. This elevated conductivity overrides the benefits of the pore water phase changes, especially if the wall is exposed to high outdoor temperatures which cause the unfired earth to dry out. A significant improvement of performance is however achieved by increasing the earth porosity through the application of a lower compaction effort, thus leading to lower levels of thermal conductivity.
- ***Effect of embedded hemp fibres.*** The hypercompacted unfired full bricks incorporating hemp fibres exhibit marginally lower densities than the hypercompacted unfired full bricks without fibres. Despite this ostensibly similar density, the presence of insulating fibres produces a remarkable enhancement of thermal performance at wall scale. Interestingly, this improvement is achieved with a relatively low content of hemp fibres corresponding to only 1.5% in dry mass.
- ***Effect of brick holes.*** The best thermal performance is observed for the wall made of hypercompacted unfired hollow bricks. This is because of the presence of air pockets inside the brick holes, which strongly hinders the exchange of heat between outdoor and indoor environments.

Based on the above conclusions, thermal performance at wall scale could be optimised by making use of lightly compacted unfired hollow bricks that incorporate hemp fibres. These bricks would combine the benefit of a low material density, and hence a low thermal conductivity, together with the advantages of a high thermal inertia associated to the phase changes of pore water and the additional insulation provided by hemp fibres and air pockets. The manufacture of such optimised

bricks represents a potential development of the present work and will be the object of future research.

Finally, the results from the present campaign provide an experimental database that can be used for validating computational models of raw earth buildings and therefore promoting the use of earthen materials in construction practice.

ACKNOWLEDGEMENT

The financial contribution of the "Agglomération Côte Basque Adour" through the project "Performances hygrothermiques et durabilité de briques de terre crue pour l'écoconstruction" is gratefully acknowledged.

REFERENCES

1. AFNOR (1991). NF P 94-054; Soils: investigation and testing – Determination of particle density- Pycnometer method.
2. AFNOR (1992). NF P 94-057. Soils: investigation and testing – Granulometric analysis – Hydrometer method.
3. AFNOR (1993). NF P 94-051; Soils: Investigation and testing – Determination of Atterberg's limits – Liquid limit test using Casagrande apparatus – Plastic limit test on rolled thread.
4. AFNOR (1995). NF P 94-050. Soils: investigation and testing – Determination of the moisture content – Oven drying method.
5. AFNOR (1995). XP P 94-041. Soils: investigation and testing – Granulometric description – Wet sieving method.
6. AFNOR (1999). NF P 94-093. Soils : Investigation and testing — Determination of the compaction characteristics of a soil — Standard Proctor test — Modified Proctor test.
7. AFNOR (2006). NF EN 196-1. Methods of testing cement – Determination of strength of cement mortar.
8. Allinson, D., & Hall, M. (2010). Hygrothermal analysis of a stabilised rammed earth test building in the UK. Energy and Buildings, 42(6), 845-852.
9. Aste, N., Angelotti, A., & Buzzetti, M. (2009). The influence of the external walls thermal inertia on the energy performance of well insulated buildings. Energy and buildings, 41(11), 1181-1187.
10. Brick Industry Association (2006). Manufacturing of brick. Technical notes on Brick Construction. Reston, Virginia.
11. Bruno, A. W. (2016). *Hygro-mechanical characterisation of hypercompacted earth for building construction* (Doctoral dissertation, Ph. D. Université de Pau et des Pays de l'Adour).
12. Bruno, A. W., Gallipoli, D., Perlot, C., & Mendes, J. (2017a). Mechanical behaviour of hypercompacted earth for building construction. *Materials and Structures*, 50(2), 160.

13. Bruno, A. W., Gallipoli, D., Perlot, C., & Mendes, J. (2017b). Effect of stabilisation on mechanical properties, moisture buffering and water durability of hypercompacted earth. *Construction and Building Materials*, 149, 733-740.
14. Bruno, A. W., Gallipoli, D., Perlot, C., & Mendes, J. (2019). Optimization of bricks production by earth hypercompaction prior to firing. *Journal of Cleaner Production*, 214, 475-482.
15. Bruno, A. W., Perlot, C., Mendes, J., & Gallipoli, D. (2018). A microstructural insight into the hygro-mechanical behaviour of a stabilised hypercompacted earth. *Materials and Structures*, 51(1), 32.
16. Cagnon, H., Aubert, J. E., Coutand, M., & Magniont, C. (2014). Hygrothermal properties of earth bricks. *Energy and Buildings*, 80, 208-217.
17. Dao, K., Ouedraogo, M., Millogo, Y., Aubert, J. E., & Gomina, M. (2018). Thermal, hydric and mechanical behaviours of adobes stabilized with cement. *Construction and Building Materials*, 158, 84-96.
18. Demirboğa, R. (2003). Influence of mineral admixtures on thermal conductivity and compressive strength of mortar. *Energy and buildings*, 35(2), 189-192.
19. Dondi, M., Mazzanti, F., Principi, P., Raimondo, M., & Zanarini, G. (2004). Thermal conductivity of clay bricks. *Journal of materials in civil engineering*, 16(1), 8-14.
20. El Fgaier, F., Lafhaj, Z., Brachelet, F., Antczak, E., & Chapiseau, C. (2015). Thermal performance of unfired clay bricks used in construction in the north of France: Case study. *Case studies in construction materials*, 3, 102-111.
21. Fahmy, M., Mahdy, M. M., & Nikolopoulou, M. (2014). Prediction of future energy consumption reduction using GRC envelope optimization for residential buildings in Egypt. *Energy and Buildings*, 70, 186-193.
22. Fang, Z., Li, N., Li, B., Luo, G., & Huang, Y. (2014). The effect of building envelope insulation on cooling energy consumption in summer. *Energy and Buildings*, 77, 197-205.
23. Gallipoli, D., Bruno, A. W., Perlot, C., & Mendes, J. (2017). A geotechnical perspective of raw earth building. *Acta Geotechnica*, 12(3), 463-478.
24. Hall, M., & Allinson, D. (2009). Assessing the effects of soil grading on the moisture content-dependent thermal conductivity of stabilised rammed earth materials. *Applied Thermal Engineering*, 29(4), 740-747.
25. Hall, M. R., & Allinson, D. (2010). Transient numerical and physical modelling of temperature profile evolution in stabilised rammed earth walls. *Applied Thermal Engineering*, 30(5), 433-441.
26. Houben, H., & Guillaud, H. (1989). *Traité de construction en terre*. Editions Parenthèses.
27. IEA International Energy Agency (2013). *Transition to sustainable buildings: Strategies and opportunities to 2050*. OECD Publishing.
28. Indekeu, M., Woloszyn, M., Grillet, A. C., Soudani, L., & Fabbri, A. (2017). Towards hygrothermal characterization of rammed earth with small-scale dynamic methods. *Energy Procedia*, 132, 297-302.
29. Karimpour, M., Belusko, M., Xing, K., Boland, J., & Bruno, F. (2015). Impact of climate change on the design of energy efficient residential building envelopes. *Energy and Buildings*, 87, 142-154.
30. Laborel-Préneron, A., Magniont, C., & Aubert, J. E. (2018). Hygrothermal properties of unfired earth bricks: effect of barley straw, hemp shiv and corn cob addition. *Energy and Buildings*, 178, 265-278.
31. Li, J., Cao, W., & Chen, G. (2015). The heat transfer coefficient of new construction–Brick masonry with fly ash blocks. *Energy*, 86, 240-246.

32. Li, H., Xiao, H. G., & Ou, J. P. (2004). A study on mechanical and pressure-sensitive properties of cement mortar with nanophase materials. *Cement and Concrete research*, 34(3), 435-438.
33. Little, B., & Morton, T. (2001). *Building with earth in Scotland: Innovative design and sustainability*. Edinburgh: Scottish Executive Central Research Unit.
34. Maillard, P., & Aubert, J. E. (2014). Effects of the anisotropy of extruded earth bricks on their hygrothermal properties. *Construction and Building Materials*, 63, 56-61.
35. Mazhoud, B., Collet, F., Pretot, S., & Lanos, C. (2018). Development and hygric and thermal characterization of hemp-clay composite. *European Journal of Environmental and Civil Engineering*, 22(12), 1511-1521.
36. McGregor, F., Heath, A., Fodde, E., & Shea, A. (2014). Conditions affecting the moisture buffering measurement performed on compressed earth blocks. *Building and Environment*, 75, 11-18.
37. McGregor, F., Heath, A., Maskell, D., Fabbri, A. and Morel, J.C. (2016). A review on the buffering capacity of earth building materials. *Proceedings of the Institution of Civil Engineers – Construction Materials*. DOI: 10.1680/jcoma.15.00035
38. Medjelekh, D., Ulmet, L., Gouny, F., Fouchal, F., Nait-Ali, B., Maillard, P., & Dubois, F. (2016). Characterization of the coupled hygrothermal behavior of unfired clay masonries: Numerical and experimental aspects. *Building and Environment*, 110, 89-103.
39. Mirrahimi, S., Mohamed, M. F., Haw, L. C., Ibrahim, N. L. N., Yusoff, W. F. M., & Aflaki, A. (2016). The effect of building envelope on the thermal comfort and energy saving for high-rise buildings in hot–humid climate. Renewable and Sustainable Energy Reviews, 53, 1508-1519.
40. Morel, J. C., Mesbah, A., Oggero, M., & Walker, P. (2001). Building houses with local materials: means to drastically reduce the environmental impact of construction. *Building and Environment*, 36(10), 1119-1126.
41. Pacheco-Torgal, F., & Jalali, S. (2012). Earth construction: Lessons from the past for future eco-efficient construction. *Construction and building materials*, 29, 512-519.
42. Papadopoulos, A. M. (2005). State of the art in thermal insulation materials and aims for future developments. *Energy and Buildings*, 37(1), 77-86.
43. Rode, C., Peuhkuri, R. H., Mortensen, L. H., Hansen, K. K., Time, B., Gustavsen, A., ... & Harderup, L. E. (2005). *Moisture buffering of building materials*. Technical University of Denmark, Department of Civil Engineering.
44. Rohen, L. A., Neves, A. C., Mantovani, D. D. P., Maurício, F. C., da Silva Vieira, J., Pontes, L. D. A., ... & Monteiro, S. (2017). Hemp Fiber Density Using the Pycnometry Technique. In *Characterization of Minerals, Metals, and Materials 2017* (pp. 423-428). Springer, Cham.
45. Serrano, S., de Gracia, A., & Cabeza, L. F. (2016). Adaptation of rammed earth to modern construction systems: Comparative study of thermal behavior under summer conditions. *Applied energy*, 175, 180-188.
46. Soudani, L., Fabbri, A., Morel, J. C., Woloszyn, M., Chabriac, P. A., Wong, H., & Grillet, A. C. (2016). Assessment of the validity of some common assumptions in hygrothermal modeling of earth based materials. *Energy and Buildings*, 116, 498-511.
47. Soudani, L., Woloszyn, M., Fabbri, A., Morel, J. C., & Grillet, A. C. (2017). Energy evaluation of rammed earth walls using long term in-situ measurements. *Solar Energy*, 141, 70-80.
48. Stazi, F., Tomassoni, E., Bonfigli, C., & Di Perna, C. (2014). Energy, comfort and environmental assessment of different building envelope techniques in a Mediterranean climate with a hot dry summer. *Applied energy*, 134, 176-196.

49. The Concrete Block Association (2017). Aggregate Concrete Blocks. Datasheet 14. Web link: https://www.cba-blocks.org.uk/wp-content/uploads/2018/03/CBA-2pp-Cellular-Blocks-datasheet-rnd2.pdf (Last visited: 21/08/2017)
50. Tinsley, J., & Pavía, S. (2019). Thermal performance and fitness of glacial till for rammed earth construction. *Journal of Building Engineering*, 24, 100727.
51. Wang, X., Zhang, Y., Xiao, W., Zeng, R., Zhang, Q., & Di, H. (2009). Review on thermal performance of phase change energy storage building envelope. *Chinese science bulletin*, 54(6), 920-928.